Valence band offsets for CuI on (-201) bulk Ga_2O_3 and epitaxial (010) $(Al_{0.14}Ga_{0.86})_2O_3$

Chaker Fares, F. Ren, David C. Hays, B. P. Gila, Marko Tadjer, Karl D. Hobart, and S. J. Pearton

Citation: Appl. Phys. Lett. **113**, 182101 (2018); doi: 10.1063/1.5055941
View online: https://doi.org/10.1063/1.5055941
View Table of Contents: http://aip.scitation.org/toc/apl/113/18
Published by the American Institute of Physics

Valence band offsets for CuI on (-201) bulk Ga_2O_3 and epitaxial (010) $(Al_{0.14}Ga_{0.86})_2O_3$

Chaker Fares,[1] F. Ren,[1] David C. Hays,[2] B. P. Gila,[2,3] Marko Tadjer,[4] Karl D. Hobart,[4] and S. J. Pearton[3,a)]
[1]*Department of Chemical Engineering, University of Florida, Gainesville, Florida 32611, USA*
[2]*Nanoscale Research Facility, University of Florida, Gainesville, Florida 32611, USA*
[3]*Department of Materials Science and Engineering, University of Florida, Gainesville, Florida 32611, USA*
[4]*US Naval Research Laboratory, Washington, DC 20375, USA*

(Received 12 September 2018; accepted 18 October 2018; published online 29 October 2018)

Thin films of copper iodide (CuI) were grown on (-201) bulk Ga_2O_3 and (010) epitaxial $(Al_{0.14}Ga_{0.86})_2O_3$ using a copper film iodination reaction method. The valence band offsets for these heterostructures were measured by X-ray photoelectron spectroscopy (XPS). High resolution XPS data of the O 1s peak and onset of elastic losses were used to establish the $(Al_{0.14}Ga_{0.86})_2O_3$ bandgap to be 5.0 ± 0.30 eV. The valence band offsets were -0.25 eV $\pm$ 0.07 eV and 0.05 ± 0.02 eV for CuI on Ga_2O_3 or $(Al_{0.14}Ga_{0.86})_2O_3$, respectively. The respective conduction band offsets were 1.25 ± 0.25 eV for Ga_2O_3 and 1.85 ± 0.35 eV for $(Al_{0.14}Ga_{0.86})_2O_3$. Thus, there is a transition from type-II to type-I alignment as Al is added to β-Ga_2O_3. The low valence band offsets are ideal for hole transport across the heterointerfaces. *Published by AIP Publishing.*
https://doi.org/10.1063/1.5055941

β-Ga_2O_3 is an attractive material for power electronic applications due to its wide bandgap, controlled n-type doping, and high quality, inexpensive substrate technology.[1–7] A wide variety of lateral and vertical transistors and rectifiers have been reported,[1,3–7] and $(Al_xGa_{1-x})_2O_3/Ga_2O_3$ heterostructures have also been demonstrated using modulation doping of the barrier layer.[8–14] There is strong interest in these heterostructures involving β-$(Al_xGa_{1-x})_2O_3$ monoclinic phase alloys, in which the bandgap can be varied from 4.8 to 6 eV.[14,15] In terms of doping of these materials, controlled n-type doping with Sn, Si, and Ge has been demonstrated, but because of the relatively flat valence band, it is likely impossible to achieve conventional p-type doping of Ga_2O_3.[16] While p-type conduction has been reported from Ga vacancies at high temperature,[17] the predicted large ionization energies for acceptor dopants, the self-trapping of holes into polarons, and the presence of common n-type impurities and native n-type defects all work against achieving p-type conduction. This asymmetry in n-type versus p-type doping is common for many wide bandgap semiconductors.[18–20] The absence of a p-type doping capability limits the type of device that can be fabricated, not only the ability to have p-n junctions but also in structures such as edge termination on power devices.

One option is to employ heterojunctions of Ga_2O_3 with p-type semiconductors such as SiC, NiO, Cu_2O, CuI, or diamond.[18–27] As an example, Watahiki *et al.*[26] employed sputtered p-Cu_2O and demonstrated 1.49 kV pn diodes with a specific on-resistance of 8.2 mΩ cm^2. Other groups have also reported heterojunctions of Ga_2O_3 with p-Cu_2O.[24,27] There is particular interest in p-type CuI,[18–25] which is a wide-gap semiconductor with a zincblende-type structure at ambient conditions, used as a transparent electrode for improving hole collection in organic solar cells and also for forming a heterojunction with n-type oxides. Koehler *et al.*[25] reported the p-CuI/n-Ga_2O_3 rectifying heterojunction with an on/off ratio of $>10^4$ measured at room temperature, with ideality factor $n = 1.18$ as the junction turned on at higher bias. The current-voltage-temperature measurements degraded the junction, indicative of CuI oxidation and need for passivation.[25] More work is needed to understand the characteristics of this system. In this letter, we report the band alignment for CuI on both Ga_2O_3 and $(Al_{0.14}Ga_{0.86})_2O_3$ and find low barriers to hole transport.

The CuI films were grown in a two-step process.[18–25] First, Cu was deposited by RF magnetron sputtering on Ga_2O_3 and $(Al_{0.14}Ga_{0.86})_2O_3$ at room temperature using a 3-in. diameter target of pure (6N) copper. The RF power was 90 W, and the working pressure was 5 mTorr in pure Ar ambient (50 sccm flow rate). The dc bias on the electrode under these conditions is ~30–40 V. The samples were cleaned prior to deposition using rinses of acetone and isopropyl alcohol (IPA), N_2 drying, and finally O_3 exposure for 15 min. The commercial bulk β-phase Ga_2O_3 single crystals with the (-201) surface orientation (Tamura Corporation, Japan) were grown by the edge-defined-film-fed growth method. Hall data showed an n-type carrier concentration of $\sim 3 \times 10^{17}$ cm^{-3}. The $(Al_{0.14}Ga_{0.86})_2O_3$ was grown by Molecular Beam Epitaxy onto bulk (010) β-Ga_2O_3 substrates that were Sn-doped (6.3×10^{18} cm^{-3}). These Aluminum Gallium Oxide (AGO) layers were doped with Si to produce an n-type carrier density of 10^{17} cm^{-3} determined by electrochemical capacitance-voltage measurements and were 55 nm thick. After the Cu deposition, the samples were placed in a Petri dish cover and mounted with a Teflon holder. 99.999% iodine particles were placed into the Petri dish and then heated to 120 °C for 5 min using a hotplate. This forms a textured (111) film with a lattice parameter of 6.0546 Å.

a)Author to whom correspondence should be addressed: spear@mse.ufl.edu

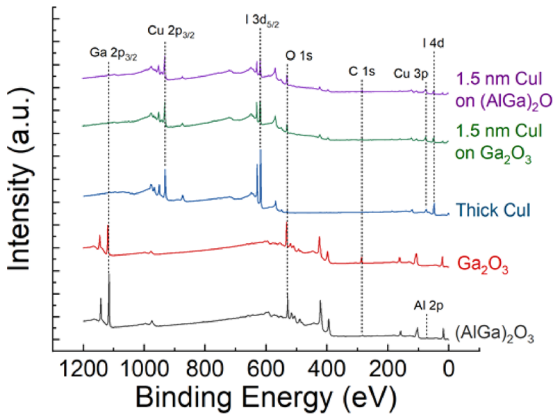

FIG. 1. XPS survey scans of thick CuI, 1.5 nm CuI on $(Al_{0.14}Ga_{0.86})_2O_3$, 1.5 nm CuI on Ga_2O_3, a reference Ga_2O_3 sample, and a $(Al_{0.14}Ga_{0.86})_2O_3$ reference sample. The intensity is in arbitrary units (a.u.).

Koehler *et al.*[25] reported a carrier concentration of $2 \times 10^{18}\,cm^{-3}$ and a mobility of $\sim 7\,cm^2/V\,s$ under these conditions. Two types of CuI films were formed—thin layers (1.5 nm) on the oxide samples and thick layers (150 nm) as references.

After iodination of Cu, the samples were directly placed into the XPS system to minimize oxidation of CuI. XPS survey scans were used to obtain the chemical state of CuI, Ga_2O_3, and β-$(Al_{0.14}Ga_{0.86})_2O_3$ and identify peaks for high resolution analysis.[28–33] An ULVAC PHI XPS with a monochromatic, Al X-ray source (energy 1486.6 eV) at a source power of 300 W was used. The analysis area was 10 μm in diameter, while a take-off angle of 50° and an acceptance angle of ±7° were utilized. The electron pass energy was 23.5 eV for the high-resolution scans and 93.5 eV for the survey scans. The approximate escape depth ($3\lambda \sin\theta$) of the electrons was 80 Å. In this system, all of the peaks are well-defined.

Charge compensation was performed using a dual beam charge neutralization system (low-energy electron beam and ion beam) to prevent charge buildup during data collection. The charge neutralization system is often not sufficient at eliminating all surface charge, and additional corrections must be performed. Using the known position of the adventitious carbon (C-C) line in the C 1s spectra at 284.8 eV, charge correction was performed. The samples and electron analyzers were electrically grounded to provide a common reference Fermi level. Differential charging was minimized with the use of an electron gun, verified using calibrations with and without the gun.[31] Since CuI is conducting and the oxide samples are doped, we would not expect significant differential charging and no time-dependence of peak position was observed. We also checked by measuring the full-width at half maximum of the core level peaks that over-compensation during charge neutralization was not present.[34]

Reflection electron energy loss spectroscopy (REELS)[35] was employed to measure the bandgap of Ga_2O_3. By taking a linear fit to the leading plasmon peak and finding its zero energy with the background, a direct measurement of valence to conduction band energy was made. REELS spectra were obtained using a 1 kV electron beam and the hemispherical electron analyzer. The bandgap of $(Al_{0.14}Ga_{0.86})_2O_3$ was determined from XPS O1s based electron energy loss measurements. The bandgap of CuI was assumed to be

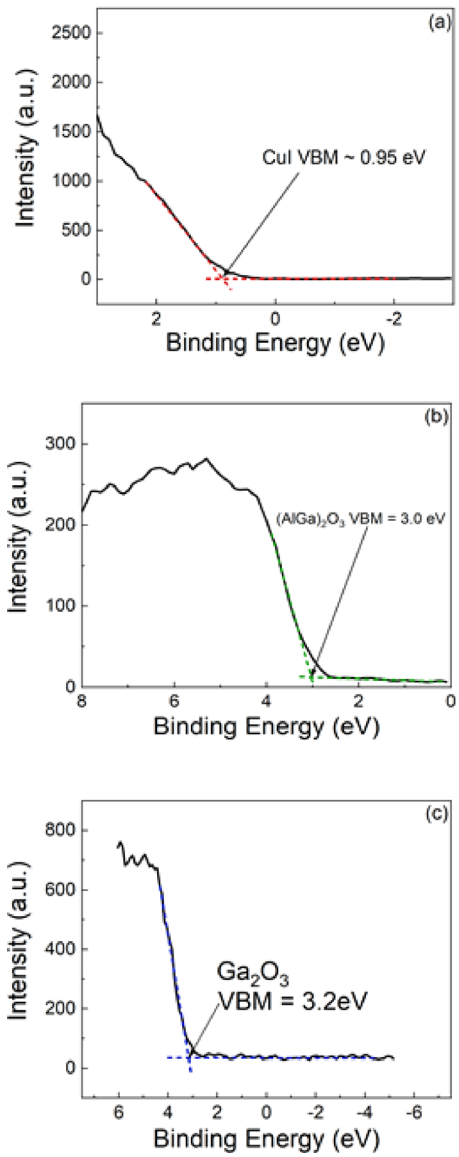

FIG. 2. XPS spectra of core levels to valence band maximum (VBM) for (a) thick CuI, (b) reference $(Al_{0.14}Ga_{0.86})_2O_3$, and (c) reference Ga_2O_3. The intensity is in arbitrary units (a.u.).

3.1 ± 0.1 eV based on the many previously published reports.[18–25] A slight deviation in the actual CuI bandgap could marginally affect conduction band offset values.

XPS confirmed the presence of CuI, with Cu in the +1 oxidation state (Cu 2p) and iodine in the −1 oxidation state (I 3d) based on the binding energies. The Cu 3p and iodine 4d showed that CuI was stoichiometric throughout the top 20 nm of the film, indicating that during synthesis, the iodine vapor reacts with more than just the Cu surface and creates a uniform CuI film.

Figure 1 shows the stacked XPS survey scans of thick (150 nm) CuI, 1.5 nm CuI on β-Ga_2O_3 or $(Al_{0.14}Ga_{0.86})_2O_3$, and the Ga_2O_3 and $(Al_{0.14}Ga_{0.86})_2O_3$ reference samples. Only the expected elements are present, indicating no gross contamination or oxidation of CuI.

The valence band maximum (VBM) was determined by linearly fitting the leading edge of the valence band and the flat energy distribution from the XPS measurements[31,33] and finding the intersection of these two lines, as shown in Fig. 2 for the thick CuI and the reference $(Al_{0.14}Ga_{0.86})_2O_3$ and Ga_2O_3.

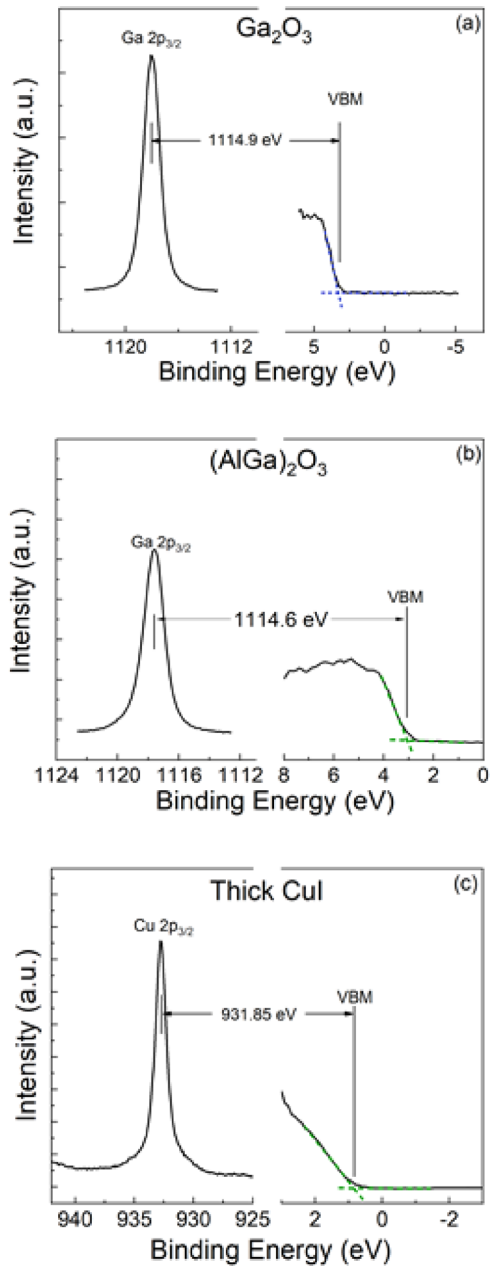

FIG. 3. High resolution XPS spectra for the vacuum-core delta regions of (a) Ga_2O_3, (b) $(Al_{0.14}Ga_{0.86})_2O_3$, and (c) thick CuI. The intensity is in arbitrary units (a.u.).

The VBMs were measured to be 0.95 ± 0.15 eV for CuI, 3.0 ± 0.2 eV for β-$(Al_{0.14}Ga_{0.86})_2O_3$, and 3.20 eV $\pm$ 0.3 eV for Ga_2O_3.

The measured bandgap of β-Ga_2O_3 from the REELS data was 4.6 ± 0.2 eV.[31] This was similar to the value obtained from XPS measurements of the type used for the alloy bandgap determination. For $(Al_{0.14}Ga_{0.86})_2O_3$, the

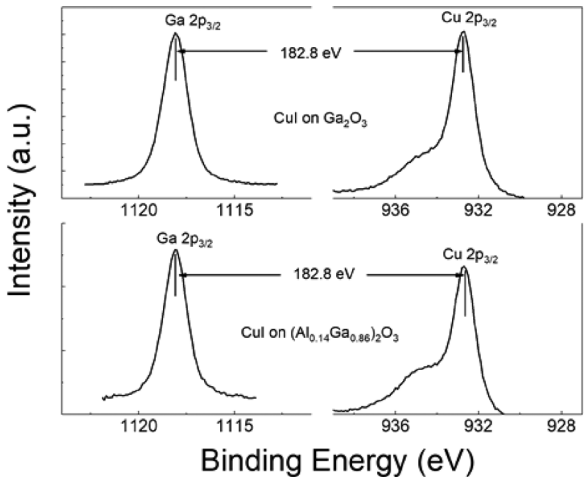

FIG. 4. High resolution XPS spectra for the CuI to Ga_2O_3 and $(Al_{0.14}Ga_{0.86})_2O_3$ core delta regions. The intensity is in arbitrary units (a.u.).

bandgap was determined to be 5.0 ± 0.3 eV, from XPS O1s based electron energy loss measurements. This is consistent with previous work on powdered samples of $(Al_xGa_{1-x})_2O_3$ over the composition range x = 0–0.4.[15] If we use the theoretical relationship derived by Peelaers *et al.*,[14] we would expect a bandgap of 5.14 eV at our composition of x = 0.14, close to the measured result. The differences in bandgaps between CuI and β-$(Al_{0.14}Ga_{0.86})_2O_3$ and β-Ga_2O_3 are therefore 1.9 and 1.5 eV, respectively.

To determine the band alignment and valence band offsets, we used the standard core level spectra approach,[32] which measures a core level and the valence band edge for each material and the shift of the core levels when the two materials have formed a heterojunction. The valence band offset is obtained from[32]

$$\Delta E_V = \left(E^1_{core} - E^1_{VBM}\right) - \left(E^2_{core} - E^2_{VBM}\right) - \left(E^1_{core} - E^2_{core}\right).$$

It is important to use a well-defined core level since the offsets are small compared to the core level energy and more deviation is expected at higher core level energies.

High resolution XPS spectra of the VBM-core delta region are shown in Fig. 3 for the β-Ga_2O_3, β-$(Al_{0.14}Ga_{0.86})_2O_3$ and thick CuI samples. These were used to determine the selected core level peak positions. Figure 4 shows the XPS spectra for the β-Ga_2O_3 and β-$(Al_{0.14}Ga_{0.86})_2O_3$ to CuI core delta regions of the heterostructure samples. These values are summarized in Table I and were then used to calculate ΔEv.

Figure 5 shows the measured band alignments of the CuI/β-Ga_2O_3 and CuI/β-$(Al_{0.14}Ga_{0.86})_2O_3$ heterostructures. The latter is a nested, type I system, while the former is a staggered

TABLE I. Summary of measured core levels in these experiments (eV).

Reference					Reference CuI				Thin CuI on Ga_2O_3 or $(AlGa)_2O_3$	
Substrate	Core level	VBM	Core level peak	Core−VBM	Core level	VBM	Core level peak	Core−VBM	Δ Core level Ga $2p_{3/2}$–Cu2p3	Valence band offset
Ga_2O_3	$Ga2p_{3/2}$	3.20	1118.10	1114.90	Cu 2p3	0.95	932.8	931.85	182.8	0.25
$(AlGa)_2O_3$	$Ga2p_{3/2}$	3.00	1117.60	1114.60	Cu 2p3	0.95	932.8	931.85	182.8	−0.05

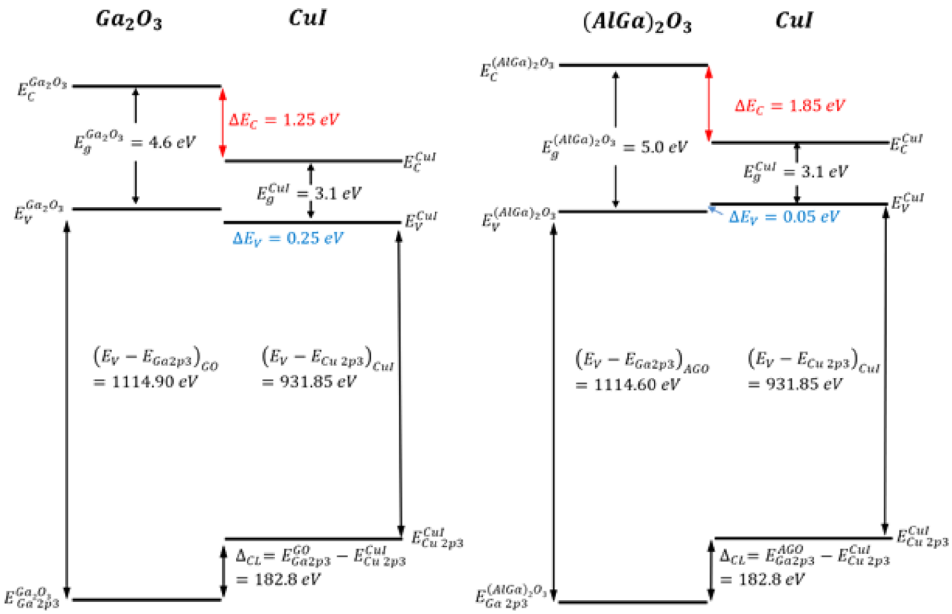

FIG. 5. Band diagrams for CuI on Ga_2O_3 (left) and CuI on $(Al_{0.14}Ga_{0.86})_2O_3$ (right).

gap type-II alignment. The valence band offset is -0.25 ± 0.07 eV, and the conduction band offset is 1.25 ± 0.25 eV for CuI/β-Ga_2O_3. For the CuI/β-$(Al_{0.14}Ga_{0.86})_2O_3$ heterostructure, the values are 0.05 ± 0.02 eV for the valence band offset and 1.85 ± 0.35 eV for the conduction band offset. These were obtained using the differences in bandgaps and the directly measured valence band offset, i.e., $\Delta E_C = E_g^{AlGaO\ or\ Ga2O3} - E_g^{CuI} - \Delta E_V$. The shift from the pure binary to the β-$(Al_xGa_{1-x})_2O_3$ alloy with a relatively low Al content is enough to shift the alignment type, but note that the energy barriers to hole transport are small in both cases and auger well for the prospects of high quality p-n heterojunctions of CuI with both Ga_2O_3 and $(Al_xGa_{1-x})_2O_3$.

In conclusion, the band alignment for CuI on Ga_2O_3 and $(Al_{0.14}Ga_{0.86})_2O_3$ is favorable for hole transport across the heterointerface and the low processing temperature is attractive for minimizing the formation of interface states. Electrical measurements are needed to demonstrate minority carrier injection at low biases in heterojunction samples.

The project or effort depicted was partially sponsored by the Department of the Defense, Defense Threat Reduction Agency, HDTRA1-17-1-011, monitored by Jacob Calkins. The content of the information does not necessarily reflect the position or the policy of the federal government, and no official endorsement should be inferred. Research at NRL was supported by the Office of Naval Research.

[1]M. J. Tadjer, N. A. Mahadik, J. A. Freitas, E. R. Glaser, A. D. Koehler, L. E. Luna, B. N. Feigelson, K. D. Hobart, F. J. Kub, and A. Kuramata, Proc. SPIE **10532**, 1053212 (2018).
[2]S. Okur, G. S. Tompa, N. Sbrockey, T. Salagaj, V. Blank, B. Henninger, M. Baldini, G. Wagner, Z. Galazka, Y. Yao, J. Rokholt, R. F. Davis, L. M. Porter, and A. Belkind, Vac. Technol. Coat. **18**(5), 31–39 (2017).
[3]S. J. Pearton, J. Yang, P. H. Cary IV, F. Ren, J. Kim, M. J. Tadjer, and M. A. Mastro, Appl. Phys. Rev. **5**, 011301 (2018).
[4]M. Higashiwaki and G. H. Jessen, Appl. Phys. Lett. **112**, 060401 (2018).
[5]M. Higashiwaki, K. Sasaki, H. Murakami, Y. Kumagai, A. Koukitu, A. Kuramata, T. Masui, and S. Yamakosh, Semicond. Sci. Technol. **31**, 034001 (2016).
[6]J. F. McGlone, Z. Xia, Y. Zhang, C. Joishi, S. Lodha, S. Rajan, S. A. Ringel, and A. R. Arehart, IEEE Electron Dev. Lett. **39**, 1042 (2018).
[7]K. D. Chabak, J. P. McCandless, N. A. Moser, A. J. Green, K. Mahalingam, A. Crespo, N. Hendricks, B. B. Howe, S. E. Tetlak, K. Leedy, R. C. Fitch, D. Wakimoto, K. Sasaki, A. Kuramata, and G. H. Jessen, IEEE Electron Device Lett. **39**, 67 (2018).
[8]Y. Zhang, A. Neal, Z. Xia, C. Joishi, J. M. Johnson, Y. Zheng, S. Bajaj, M. Brenner, D. Dorsey, K. Chabak, G. Jessen, J. Hwang, S. Mou, J. P. Heremans, and S. Rajan, Appl. Phys. Lett. **112**, 173502 (2018).
[9]S. Krishnamoorthy, Z. Xia, C. Joishi, Y. Zhang, J. McGlone, J. Johnson, M. Brenner, A. R. Arehart, J. Hwang, and S. Lodha, Appl. Phys. Lett. **111**, 023502 (2017).
[10]T. Oshima, Y. Kato, N. Kawano, A. Kuramata, S. Yamakoshi, S. Fujita, T. Oishi, and M. Kasu, Appl. Phys. Express **10**, 035701 (2017).
[11]Y. Oshima, E. Ahmadi, S. C. Badescu, F. Wu, and J. S. Speck, Appl. Phys. Express **9**, 061102 (2016).
[12]Y. Zhang, C. Joishi, Z. Xia, M. Brenner, S. Lodha, and S. Rajan, Appl. Phys. Lett. **112**, 233503 (2018).
[13]R. Wakabayashi, M. Hattori, K. Yoshimatsu, K. Horiba, H. Kumigashira, and A. Ohtomo, Appl. Phys. Lett. **112**, 232103 (2018).
[14]H. Peelaers, J. B. Varley, J. S. Speck, and C. G. Van de Walle, Appl. Phys. Lett. **112**, 242101 (2018).
[15]B. W. Krueger, C. S. Dandeneau, E. M. Nelson, S. T. Dunham, F. S. Ohuchi, and M. A. Olmstead, J. Am. Ceram. Soc. **99**, 2467 (2016).
[16]A. Kyrtsos, M. Matsubara, and E. Bellotti, Appl. Phys. Lett. **112**, 032108 (2018).
[17]E. Chikoidze, A. Fellous, A. Perez-Tomas, G. Sauthier, T. Tchelidze, C. Ton-That, T. T. Huynh, M. Phillips, S. Russell, M. Jennings, B. Berini, F. Jomard, and Y. Dumont, Mater. Today Phys. **3**, 118 (2017).
[18]M. Grundmann, F. L. Schein, M. Lorenz, T. Böntgen, J. Lenzner, and H. V. Wenckstern, Phys. Status Solidi A **210**, 1671 (2013).
[19]M. Grundmann, F. Klupfel, R. Karsthof, P. Schlupp, F.-L. Schein, D. Splith, C. Yang, S. Bitter, and H. von Wenckstern, J. Phys. D: Appl. Phys. **49**, 213001 (2016).
[20]A. Pishtshev and S. Zh. Karazhanov, J. Chem. Phys. **146**, 064706 (2017).
[21]A. Liu, H. Zhu, W.-T. Park, S.-J. Kang, Y. Xu, M.-G. Kim, and Y.-Y. Noh, Adv. Mater. **30**, 1802379 (2018).
[22]F. L. Schein, H. V. Wenckstern, and M. Grundmann, Appl. Phys. Lett. **102**, 092109 (2013).
[23]C. Yang, M. Kneil, F. L. Schein, M. Lorenz, and M. Grundmann, Sci. Rep. **6**, 21937 (2016).
[24]M. J. Tadjer, L. E. Luna, E. R. Cleveland, K. D. Hobart, and F. J. Kub, ECS Trans. **85**, 21 (2018).
[25]A. D. Koehler, M. J. Tadjer, J. G. Gallagher, G. G. Jernigan, K. D. Hobart, and F. J. Kub, in 45th International Symposium on Compound Semiconductors, Boston, MA, 1 June (2018).
[26]T. Watahiki, Y. Yuda, A. Furukawa, M. Yamamuka, Y. Takiguchi, and S. Miyajima, Appl. Phys. Lett. **111**, 222104 (2017).
[27]T. Minami, Y. Nishi, and T. Miyata, Appl. Phys. Express **6**, 044101 (2013).
[28]Z. Feng, Q. Feng, J. Zhang, X. Li, F. Li, L. Huang, H.-Y. Chen, H.-L. Lu, and Y. Hao, Appl. Surf. Sci. **434**, 440 (2018).

[29]T. Kamimura, K. Sasaki, M. H. Wong, D. Krishnamurthy, A. Kuramata, T. Masui, S. Yamakoshi, and M. Higashiwaki, Appl. Phys. Lett. **104**, 192104 (2014).
[30]V. D. Wheeler, D. I. Shahin, M. J. Tadjer, and C. R. Eddy, Jr., ECS J. Solid State Sci. Technol. **6**, Q3052 (2017).
[31]P. H. Carey, F. Ren, D. C. Hays, B. P. Gila, S. J. Pearton, S. Jang, and A. Kuramata, J. Vac. Sci. Technol., B **35**, 041201 (2017).
[32]E. A. Kraut, R. W. Grant, J. R. Waldrop, and S. P. Kowalczyk, Phys. Rev. Lett. **44**, 1620 (1980).
[33]E. Bersch, M. Di, S. Consiglio, R. D. Clark, G. J. Leusink, and A. C. Diebold, J. Appl. Phys. **107**, 043702 (2010).
[34]S. A. Chambers, L. Qiao, T. C. Droubay, T. C. Kaspar, B. W. Arey, and P. V. Sushko, Phys. Rev. Lett. **107**, 206802 (2011).
[35]H. C. Shin, D. Tahir, S. Seo, Y. R. Denny, S. K. Oh, H. J. Kang, S. Heo, J. G. Chung, J. C. Lee, and S. Tougaard, Surf. Interface Anal. **44**, 623 (2012).